arXiv:astro-ph/0212398v1 18 Dec 2002

Petschek-like reconnection with current-driven anomalous resistivity and its application to solar flares

Dmitri A. Uzdensky

Kavli Institute for Theoretical Physics, University of California

Santa Barbara, CA 93106

uzdensky@kitp.ucsb.edu

February 2, 2008

ABSTRACT

Recent numerical simulations of magnetic reconnection in two dimensions have shown that, when the resistivity is strongly localized, the reconnection region develops a Petschek-like structure, with the width of the inner diffusion region being of the order of the resistivity localization scale. In this paper, we combine this fact with a realistic model for locally-enhanced anomalous resistivity generated by current-driven microturbulence. The result is a qualitative model of the reconnection layer where the size of Petschek's diffusion region and, therefore, the final reconnection rate are determined self-consistently in terms of the main parameters of the functional dependence of anomalous resistivity on the electric current density. We then consider anomalous resistivity due to ion-acoustic turbulence as a particular case. This enables us to express the reconnection region's parameters directly in terms of the basic parameters of the plasma. Finally, we apply this reconnection model to solar flares and obtain specific predictions for typical reconnection times, which are very consistent with observations.

Subject headings: MHD — Sun: flares — Sun: magnetic fields

1. Introduction

Magnetic reconnection is a basic plasma physics phenomenon of tremendous importance in many astrophysical systems (Tsuneta 1996; Kulsrud 1998), as well as in some laboratory plasma devices (Yamada et al. 1997), including tokamaks (Kadomtsev 1975; Yamada et al.

1994). It has been studied extensively over the past five decades (e.g., Giovannelli 1946; Vasyliunas 1975; Biskamp 2000). Historically, the first (and perhaps still the most important) application of magnetic reconnection has been to explain the solar flare phenomenon, and it is in this context that the earliest reconnection models have been developed.

The first theoretical model of magnetic reconnection was developed by Sweet (1958) and by Parker (1957, 1963). In this model, magnetic field is frozen into the plasma everywhere except in a very thin layer where the current density is so high that resistive effects become important no matter how small the resistivity is. It is inside this thin current layer that the actual breaking (and reconnecting) of the magnetic lines of force takes place, accompanied by a violent release of enormous amounts of magnetically stored energy, thus leading to the observed flare. The Sweet–Parker theory predicts that the current layer thickness, $\delta_{\rm SP}$, scale as $\delta_{\rm SP} \sim L/\sqrt{S}$, where L is the global system size (typically of order 10^9 cm in the solar corona) and $S \equiv LV_A/\eta$ is the global Lundquist number (here V_A is the Alfvén velocity and η is the magnetic diffusivity; in the rest of this paper we shall refer to η as the resistivity). Correspondingly, the typical reconnection timescale is found to be $\tau_{\rm rec} \sim \tau_A(L)\sqrt{S}$, where $\tau_A(L) \equiv L/V_A$ is the global Alfvén transit time. It has been immediately realized that the resulting reconnection time turns out to be too long; in the solar corona one typically has $S \sim 10^{12} - 10^{14}$ and $\tau_A(L) \sim 1$ sec, which leads to $\tau_{\rm rec}$ of the order of a few months. This is in sharp contrast with the typical observed solar flare duration of order $10^2 - 10^3$ sec. Thus, since its early years, the main thrust of magnetic reconnection research has been to explain reconnection rates that are much faster than the Sweet–Parker theory predicts.

Starting from the 1960s, two major routes toward faster reconnection were proposed. One of them was to use the so-called *anomalous resistivity* instead of the classical Spitzer resistivity used in the original Sweet–Parker model (Coppi & Friedland 1971; Smith & Priest 1972; Coroniti & Eviatar 1977; Kulsrud 1998). The idea was that, as a current layer forms, its thickness becomes so small, and hence the current density becomes so high, that the drift velocity of the current-carrying electrons exceeds a certain threshold, such as the ion-sound or the electron thermal speed. This leads to the excitation of current-driven kinetic microturbulence, which, in turn, provides a more efficient (compared to particle-particle collisions) mechanism for the scattering of electrons (via wave-particle interactions). As a result, one ends up with a greatly enhanced effective resistivity and, hence, a greatly reduced effective Lundquist number. When substituted into the Sweet–Parker scaling, this results in a greatly enhanced reconnection rate. In fact, controlled laboratory studies of magnetic reconnection have shown a good agreement with a simple Sweet–Parker model augmented with some (experimentally measured) anomalously enhanced resistivity (Ji et al. 1998, 1999). On the other hand, in the solar flare context, the Sweet–Parker model with anomalous resistivity gives typical reconnection times of the order of several hours (e.g.,

Kulsrud 1998), a great improvement over Spitzer resistivity. Among various anomalous resistivity mechanisms, the one most frequently quoted has been the *ion-acoustic turbulence* (IAT). Rapid magnetic energy dissipation due to the IAT-driven anomalous resistivity has in fact also been invoked to explain coronal heating (Rosner et al. 1978).

Another possibility leading to shorter reconnection times was proposed by Petschek (1964). His very elegant model makes use of a somewhat more complicated reconnection layer geometry, while still relying on simple resistive magnetohydrodynamics (MHD) without invoking any new physics at the microscopic level. The *Petschek model* actually does not predict a unique configuration of the reconnection layer and a unique reconnection rate. Instead, this model encompasses an entire one-parametric family of solutions. Each of these configurations has at its center a small Sweet–Parker-like layer, called the *diffusion region*, and four standing slow-mode shocks emanating from the ends of this central layer. The members of this family of solutions can be labeled by the width (or length) Δ of the inner diffusion region. As Petschek noticed, in the Sweet–Parker model the reconnection process had been slowed down by the very large aspect ratio L/δ of the reconnection layer. He suggested that the width Δ of the layer's diffusion region does not have to be as large as the global size L; if Δ can be made sufficiently short, the reconnection process will go much faster than in the Sweet–Parker model. The maximum value of Δ corresponds to the Sweet–Parker solution, which is, therefore, just one of the family members. The reconnection rate ranges from the slowest (Sweet–Parker) rate to the so-called maximum Petschek rate, which scales as $1/\log S$. We thus see that the relatively strong square-root dependence on the resistivity, characteristic for the Sweet–Parker model, is replaced here by a much weaker logarithmic dependence; even for a very large $S \sim 10^{14}$, the resulting reconnection timescale turns out to be reasonably short, of order $10^2\,\tau_A(L)$.

This model had remained the favorite model of reconnection until 1980s, when two-dimensional (2D) resistive-MHD numerical simulations by Biskamp (1986) showed that, in the case of a spatially uniform resistivity, a Petschek-like configuration fails to form and that a long (of order L) current layer tends to form instead, consistent with the Sweet–Parker picture. This finding has been confirmed in a number of numerical simulations performed by several other groups (Scholer 1989; Ugai 1992, 1999; Yokoyama & Shibata 1994; Uzdensky & Kulsrud 2000; Erkaev et al. 2000, 2001). A theoretical explanation has been put forward by Kulsrud (2001). He noticed that, when the resistivity is uniform, the relatively large transverse magnetic field that is needed to support the standing shocks in the Petschek model is rapidly swept out of the diffusion region by the downstream flow, while its regeneration due to the nonuniform merging is not fast enough. As a result, the diffusion region's size Δ (which Kulsrud calls L') increases until it reaches the global scale L and the reconnection rate, correspondingly, slows down to the usual Sweet–Parker rate. This explanation has been

confirmed numerically by Uzdensky & Kulsrud (2000) (see also Kulsrud 1998).

It has been noticed, however, that the key assumption leading to the above conclusion was the assumption of uniform resistivity (which is a very common assumption in numerical simulations in general). Simulations featuring a *non-uniform resistivity* have shown that a Petschek-like structure does form and can be stable whenever the resistivity is locally enhanced in some small region near the X-point at the center of the reconnection region (Ugai & Tsuda 1977; Sato & Hayashi 1979; Ugai 1986, 1992, 1999; Scholer 1989; Yokoyama & Shibata 1994; Erkaev et al. 2000, 2001; Ugai & Kondoh 2001; Biskamp & Schwarz 2001). A nice plausible theoretical explanation of this phenomenon has again been provided by Kulsrud (2001), who analyzed how a locally enhanced resistivity may lead to a more efficient regeneration of the transverse magnetic field through non-uniform merging and thus to the sustainment of Petschek's shocks. In addition, recent numerical work by Erkaev et al. (2000, 2001) and by Biskamp & Schwarz (2001) has shown that the particular Petschek-like configuration that forms in the localized-resistivity situation is characterized by the width Δ of the inner diffusion region being of the order of the resistivity localization scale, which in this paper we shall call l_η (Erkaev et al. 2000, 2001; Biskamp & Schwarz 2001). We thus see that resistivity-localization mechanism plays a crucial role in determining the final reconnection rate.

From the point of view of physical reality, the main motivating force behind these localized-resistivity studies has been the idea that anomalous resistivity, being such a sensitive function of the local current density, may in fact be triggered only in a small neighborhood of the X-point, where the current density is highest. In other words, anomalous resistivity can enhance reconnection rate not only directly (by simply being higher than the collisional resistivity), but also indirectly, via enabling the Petschek mechanism (by being strongly localized). This is one of the key ideas behind the so-called spontaneous fast reconnection model suggested by Ugai (1986, 1992, 1999; also see Ugai & Tsuda 1977; Yokoyama & Shibata 1994; Ugai & Kondoh 2001) on the basis of numerical simulations.

Up until now, however, with the notable exception of the work by Kulsrud (2001), there have been no analytical attempts to combine the Petschek reconnection model with any physically realistic model of anomalous resistivity, which would provide unique theoretical predictions for the main parameters of the reconnection region, such as the width of the diffusion region and the reconnection rate, in terms of the basic parameters of the plasma. The goal of this paper is to remedy this situation by attempting to build a simple theoretical framework incorporating a particular anomalous resistivity mechanism (ion-acoustic turbulence).

In § 2 we present our model of the Petschek reconnection layer with a generic form of

anomalous resistivity. In particular, in § 2.1 we describe the basic elements of the model, e.g., the Sweet–Parker relationships for the inner diffusion region and the functional dependence of anomalous resistivity, η, on the current density j. In § 2.2 we discuss possible solutions and explore their stability. In § 2.3 we calculate the reconnection rate in terms of the model parameters. § 3 is devoted to the specific case of anomalous resistivity due to the IAT; in this section we make use of the well-developed theory of ion-acoustic turbulence to express all major reconnection layer parameters, including the reconnection rate, in terms of the basic plasma parameters (such as the magnetic field strength, plasma density, and the electron and ion temperatures). We apply the obtained results to solar flare environment in § 4 and find a very reasonable agreement in terms of general timescales. We list our conclusions in § 5.

2. Model of the Reconnection Layer

2.1. Three Main Ingredients of the Model

We now describe our model of a Petschek-like reconnection configuration that is formed in the presence of anomalous resistivity due to a current-driven microturbulence. This model is semi-empirical and does not pretend to describe any real physical system in full detail. We believe, however, that it correctly captures the most critical qualitative features of the reconnection phenomenon.

Our model represents a synthesis of the following three external ingredients that are combined to build a complete and, hopefully, self-consistent description of the system:
1) the numerically-observed fact that, whenever the resistivity is strongly localized, a Petschek-like structure tends to develop, with a characteristic width of the central diffusion region being of the order of the resistivity localization scale (Erkaev et al. 2000, 2001; Biskmap & Schwarz 2001);
2) Sweet–Parker model for the central diffusion region of the Petschek configuration;
3) a physically motivated model for the anomalous resistivity.

We shall now proceed with the description and integration of these three main ingredients. Let y be the direction along the layer and x across the layer. Figure 1 shows schematically the central part of the Petschek-like configuration discussed in this paper. The shaded rectangular area (of characteristic thickness δ and width Δ) in the center of the Figure is the inner diffusion region where the electric current density is concentrated. This is the region where the effective plasma resistivity plays an important role and where the actual breaking

of magnetic field lines takes place.

For definiteness, we use Ampere's law to define the thickness δ of this central current layer in terms of the central current density $j_0 \equiv j(0,0)$ and the outside magnetic field B_0 as

$$\delta \equiv \frac{cB_0}{4\pi j_0}\,. \tag{1}$$

In addition, suppose that along the midplane $x = 0$ the current density has a certain profile $j(y)$. We define the characteristic width Δ of the diffusion region in terms of the function $j(y)$ as the distance from the center $y = 0$ to the point where the current density drops by a factor of e:

$$j(y = \Delta) = j_0/e\,. \tag{2}$$

Similarly, we define the characteristic scale l_η for the variation of the plasma resistivity $\eta(y)$ along the layer as

$$\eta(y = l_\eta) = \eta(y = 0)/e\,. \tag{3}$$

In general, the two scales Δ and l_η may be very different. However, as discussed in the introduction, recent numerical simulations have shown that, if the resistivity is strongly localized ($l_\eta \ll L$, where L is the global system size), a Petschek-like configuration develops with the width of the inner diffusion region being of order of the resistivity localization scale: $\Delta \sim l_\eta$. This important condition serves as the criterion for selecting a unique solution out of the entire family of Petschek configurations. We shall call this unique Petschek configuration an equilibrium configuration. In our present analysis we shall rely on this empirical finding as on one of the important building blocks of our model.

Note that, in general, Δ and l_η in this equilibrium Petschek configuration may differ by a finite factor, so let us define a dimensionless parameter K such that the equilibrium configuration has $\Delta = \Delta_{\rm eq} \equiv K l_\eta$. In our analysis it will actually be more convenient to use another dimensionless parameter to describe the equilibrium Petschek configuration. We shall call this parameter ξ and define it in terms of $j(y)$ as $j(l_\eta) = \xi j_0/e$. The parameters K and ξ are related to each other, but the exact relationship depends on the detailed profiles of $\eta(y)$ and $j(y)$; it is, however, unimportant for the purposes of the present paper: we shall only use the fact that, since $j(y)$ is a monotonically decreasing function of y, we have $\xi > 1$ whenever $\Delta_{\rm eq} > l_\eta$ ($K > 1$) and $\xi < 1$ whenever $\Delta_{\rm eq} < l_\eta$ ($K < 1$). We expect ξ to be of order one, its precise value depends on the details of the problem and must be determined from numerical simulations. The analysis in this paper will be restricted to a situation where $\Delta_{\rm eq}$, i.e., the equilibrium value of Δ, is somewhat greater than l_η; thus we take $\xi > 1$. This choice is made purely for reasons of convenience, as will be elucidated below.

We shall now describe the other two main components of the model. The second ingredient is the model for the inner diffusion region. In Petschek's theory, this region is a Sweet–Parker-like current layer with the thickness δ related to its width Δ via the relationship:

$$\frac{\delta}{\Delta} \simeq S_{\Delta}^{-1/2}, \tag{4}$$

where

$$S_{\Delta} \equiv \frac{V_A \Delta}{\eta_{\rm eff}} \tag{5}$$

is the Lundquist number for the scale Δ. Here we shall take $\eta_{\rm eff} = \eta(j_0)$, the resistivity at the very center of the layer. Then we can rewrite the above expression for δ as

$$\delta = \sqrt{\frac{\Delta}{V_A}\eta(j_0)}\,. \tag{6}$$

This is a very important relationship that we are going to invoke many times throughout the paper.

The next question is what actually determines the value of l_η and hence Δ. We suggest that these values have to be determined by the properties of the function $\eta(j)$. We thus need to introduce the third ingredient, namely, a physically plausible model for anomalous resistivity, expressed in terms of a single function $\eta(j)$.

Our choice of the function $\eta(j)$ is motivated by anomalous resistivity due to a current-driven microturbulence. Correspondingly, we here adopt a very simple, minimal model for $\eta(j)$, which, however, has to exhibit the following general properties: first, there exists a current-density threshold, j_c, for triggering anomalous resistivity, and second, the rapid rise of η after the threshold is exceeded stops at some large but finite value η_1, after which $\eta(j)$ continues to rise with increased j more slowly.

Thus we take $\eta(j)$ to be a prescribed function whose behavior can be described as follows (see Fig. 2):
1) For $j < j_c$, $\eta(j)$ is constant and equal to a small collisional resistivity η_0.
2) At the critical current density, $j = j_c$, η rises rapidly, essentially jumps to a value $\eta_1 \gg \eta_0$. For our convenience, we actually introduce some small finite width to this jump, $\Delta j \ll j_c$, and assume that $\eta(j)$ is a linear function in the interval $j \in [j_c, j_c + \Delta j]$. The exact value of Δj is unimportant in our analysis.
3) When j is increased even further, $j > j_c + \Delta j$, the resistivity continues to rise monotonically with increased j, but in a much slower manner.[1] In particular, we take $\eta \sim j$ in this

[1]Numerical simulations sometimes assume a stronger saturation of anomalous resistivity by imposing a strict upper limit on η (Yokoyama & Shibata 1994).

region, which is the case for ion-acoustic turbulence (e.g., Bychenkov et al. 1988). Thus we take

$$\eta(j > j_c + \Delta j) \simeq \eta_1 \frac{j}{j_c} \,. \tag{7}$$

We see that the dependence of the anomalous resistivity η on the current density j involves three parameters, j_c, η_0, and η_1. In addition to these parameters, it is convenient to introduce the critical layer thickness δ_c as a derived quantity:

$$\delta_c \equiv \frac{cB_0}{4\pi j_c} \,. \tag{8}$$

For the analysis in this section this generic level of description will suffice. In § 3, however, we shall consider a very important specific example of anomalous resistivity due to ion-acoustic turbulence and will give specific expressions for these parameters.

Here, however, we wish to make a remark concerning the manner in which we are going to use the above prescription for $\eta(j)$. In our model, η is determined solely by the local value of j. We realize, of course, that in reality the coefficients j_c, η_0, and η_1 will depend on the plasma density and temperature, and so will vary from one point to another inside the reconnection layer. In our simple reconnection model we shall, however, ignore this aspect and assume that these parameters are constant in space and time and hence the same profile $\eta(j)$ applies everywhere. In other words, η is determined solely by the local value of j.

2.2. Two possible solutions and their stability

We shall now use the $\eta(j)$ dependence shown in Figure 2 to find the correct value of j_0 that corresponds to the equilibrium Petschek solution. First, the requirement that $\Delta = Kl_\eta$ can be interpreted as follows. At $y = 0$, let us have some value j_0 and the corresponding value $\eta(j_0)$. The requirement that $j_* \equiv j(l_\eta) = \xi j_0/e$ means that $\eta(y = l_\eta) = \eta(\xi j_0/e)$. But, by definition of l_η, $\eta(y = l_\eta) = \eta(j_0)/e$. Thus, j_0 is determined using function $\eta(j)$ from the condition:

$$\eta(j_0) = e\eta(j_*) = e\eta(\xi j_0/e) \,. \tag{9}$$

The solution of this equation for a given ξ can be found by drawing a set of parabolae $\eta \propto j^\alpha$ where $\alpha = 1/(1 - \ln \xi)$, and selecting out of this set those parabolae for which the points of their intersection with the curve $\eta(j)$ are separated by a factor of e in their values of η, as shown in Figure 3. It is clearly seen from this Figure that, for any $\xi > 1$ (and, hence,

$\alpha > 1$) and for the general shape of $\eta(j)$ adopted in this paper, one finds, in principle, two such solutions.

The first solution (curve I) corresponds to j_0 lying on the rapidly rising part of the $\eta(j)$ curve, $j_0^I \in [j_c, j_c + \Delta j]$, while $j_*^I = j^I(l_\eta) = \xi j_0/e < j_c$. Then, $\eta^I(y = l_\eta) = \eta_0$ and hence $\eta^I(j_0) = e\eta_0$. We thus see that the corresponding resistivity enhancement in the inner diffusion region is not very large in this case, just by a factor e over the collisional value η_0.

The second solution (curve II) boasts much higher resistivity enhancement. In this solution, j_*^{II} falls within the narrow rapidly rising part of the $\eta(j)$ curve, and hence

$$j_0^{II} = \xi^{-1} e j_*^{II} \simeq e j_c/\xi \,. \tag{10}$$

Correspondingly, the resistivity at the center of the diffusion region is

$$\eta^{II}(j_0) = \eta(j_0^{II}) = \eta_1 e/\xi \gg \eta_0 \,. \tag{11}$$

Any Petschek-like configuration with j_0 between j_0^I and j_0^{II}, and hence with $e\eta_0 < \eta < e\eta_1/\xi$, will not be in a steady equilibrium and instead will evolve so as to increase j_0. Indeed, if $\eta(j_0) > e\eta_0$, then $\eta(j_*) > \eta_0$ and hence $j_* > j_c$. But then, since $j_0 < e j_c/\xi$, we have $j_*/j_0 > e/\xi$ and therefore $\Delta > K l_\eta$. As we know from numerical simulations, this leads to shrinkage of Δ. As we demonstrate below, this shrinkage, in turn, results in a decrease in δ and hence in an increase in j_0. The evolution will then presumably reach a stationary state when (the stable) solution II is reached.

Now, which one of the two solutions I and II will be realized in a real physical system? We suggest that, in general, the answer to this question is determined by the stability of the solutions with respect to a small change in j_0. In particular, we shall demonstrate that the first solution is unstable while the second one is stable. This will enable us to conclude that the system will evolve towards the second solution corresponding to higher η_0 and hence to a higher reconnection rate.

We shall first demonstrate that the stability properties are largely determined by the relative size of the slopes of the function $\eta(j)$ at $j = j_0$ and $j = j_* = \xi j_0/e$. We start by presenting a rather general stability analysis that works for any monotonically increasing function $\eta(j)$. Hence, in order to apply this analysis to our solution I, we need to modify our $\eta(j)$ slightly by assuming that this function has a non-zero positive (although arbitrarily small) slope $\eta'(j) > 0$ in the region $j < j_c$. We then discuss a somewhat modified treatment for the case when $\eta'(j)$ is exactly zero in this region. These modifications are not essential and the conclusion regarding solution I being unstable is the same.

So, first let us assume that $\eta'(j) \neq 0$ but has a small positive value at $j < j_c$. Let us consider an equilibrium Petschek-like configuration with $\Delta = Kl_\eta$. Let this configuration be characterized by unperturbed values δ, j_0, j_*, Δ, l_η, etc. Now, imagine that at $t = 0$ this equilibrium Petschek configuration is suddenly perturbed while preserving its Petschek-like character, that is changed into a neighboring Petschek configuration. This new Petschek configuration is, generally speaking, not in equilibrium, i.e., it does not satisfy condition (9). It will then evolve through a sequence of Petschek states. For simplicity, here we envision the process as occurring in two parts with different timescales: the adjustment between Δ and δ to conform to the Sweet–Parker structure of the diffusion region is instantaneous, whereas the adjustment of Δ to l_η occurs on a longer timescale. In reality this might not be true and these two processes may occur on the same time scale (namely, the Alfvén crossing time). But here we are only interested in the direction of the evolution, i.e., whether the perturbed system will move away or towards the equilibrium, so our qualitative analysis should be sufficient.

In particular, let us imagine that at $t = 0$ the thickness δ of the diffusion region is reduced slightly and hence the central current density is correspondingly slightly increased:

$$\delta \;\rightarrow\; \tilde{\delta} = \delta(1-\epsilon)\,, \tag{12}$$

$$j_0 \;\rightarrow\; \tilde{j_0} = j_0(1+\epsilon)\,, \tag{13}$$

where $\epsilon \ll 1$.

An increase in j_0 by a factor $(1+\epsilon)$ leads to an increase in the resistivity at the center:

$$\eta(j_0) \rightarrow \eta(\tilde{j_0}) = \eta(j_0) + \eta'(j_0) j_0 \epsilon\,. \tag{14}$$

For the system to remain a valid Petschek solution, we require that the inner diffusion region remains a Sweet–Parker layer at all times, so the width Δ of the current distribution will automatically adjust to a new value, $\tilde{\Delta}(0)$, which, according to equation (6), is

$$\Delta \rightarrow \tilde{\Delta}(0) = V_A \frac{\tilde{\delta}^2}{\eta(\tilde{j_0})} = \Delta\Big[1 - \epsilon(2 + \frac{\eta'(j_0) j_0}{\eta(j_0)})\Big] \tag{15}$$

This equation expresses the initial reduction in Δ in direct response to the reduction in δ and hence to the related increase of j_0 and $\eta(j_0)$ in the Sweet–Parker model for the diffusion region. For example, if we are considering solution I, $j_0 \in [j_c, j_c + \Delta j]$, then $\eta'(j_0) \simeq \eta_1/\Delta j \gg \eta_1/j_0 > \eta(j_0)/j_0$, and hence the last term is dominant, i.e., the initial change in Δ is mainly due to the change in resistivity:

$$\tilde{\Delta}^I(0) \simeq \Delta\Big(1 - \epsilon \frac{\eta'(j_0) j_0}{\eta(j_0)}\Big) \simeq \Delta\Big(1 - \frac{\eta_1}{\eta(j_0)} \frac{j_c}{\Delta j} \epsilon\Big) \tag{16}$$

Similarly, if we are considering solution II, then $j_0 > j_c + \Delta j$, and $\eta \propto j$ so that $\eta'(j_0) = \eta(j_0) j_0$. Then

$$\tilde{\Delta}^{II}(0) \simeq \Delta\Big(1 - 3\epsilon\Big)\,. \tag{17}$$

Let us now ask what the new value $\tilde{l}_\eta$ of the width of the enhanced-resistivity region is and how it compares with the current sheet width $\tilde{\Delta}(0)$.

From equation (14) we see that the point $y = l_\eta$ moves to a location where $\eta(y = l_\eta)$ is increased by $\eta'(j_0) j_0 \epsilon / e$ over its unperturbed value. On the other hand, this increment is equal to $\eta'(j_*)(\tilde{j_*} - j_*)$. Therefore, j_* has to increase by the amount

$$\tilde{j_*} - j_* = \frac{j_0}{e}\,\epsilon\,\frac{\eta'(j_0)}{\eta'(j_*)} = \frac{\epsilon}{\xi}\,\frac{\eta'(j_0)}{\eta'(j_*)}\,j_*\,. \tag{18}$$

We have, by combining the expressions for the changes in j_0 and j_*,

$$\frac{\tilde{j_*}}{\tilde{j_0}} = \Big(\frac{j_*}{j_0}\Big)\left[1 + \epsilon\left(\frac{1}{\xi}\,\frac{\eta'(j_0)}{\eta'(j_*)} - 1\right)\right]. \tag{19}$$

We are now going to use this result to evaluate the change in l_η.

Because of the symmetry with respect to $y = 0$, the ratio $j(y)/j_0$ should be an even function of y with the characteristic scale Δ:

$$\frac{j(y)}{j_0} = F(Y)\,, \tag{20}$$

where

$$Y \equiv \frac{y}{\Delta}\,. \tag{21}$$

Let us assume for simplicity that during the initial perturbation the shape of this function does not change. We can then write (here $Y_* \equiv l_\eta/\Delta$)

$$\frac{\tilde{j_*}}{\tilde{j_0}} \equiv F(\tilde{Y_*}) = F(Y_*)\left[1 - \mu(\tilde{Y_*} - Y_*)\right], \tag{22}$$

where

$$\mu \equiv -\frac{F'(Y)}{F(Y)}\Big|_{Y=Y_*} = -\frac{e}{\xi}\,F'(Y_*) > 0\,. \tag{23}$$

By comparing this with the above result (19) we see that the change in Y_* is equal to

$$\tilde{Y_*} - Y_* = -\frac{\epsilon}{\mu}\,\left[\frac{\eta'(j_0)}{\xi\eta'(j_*)} - 1\right]. \tag{24}$$

This equation tells us whether the ratio $Y_* = l_\eta/\Delta$ increases or decreases from its equilibrium value $1/K$. We see that the result depends on the relative sizes of the slopes of function $\eta(j)$ at $j = j_0$ and $j = j_*$. In particular, in the case of solution II, $\eta'(j_0) < \xi\eta'(j_*)$, and then it follows from equation (24) that l_η is reduced by a lesser factor than Δ. As a consequence, the resulting perturbed Petschek configuration has $\tilde{\Delta} < \tilde{\Delta}_{\rm eq} = K\tilde{l}_\eta$. We then expect, based on the results of numerical simulation mentioned above, that in this case $\tilde{\Delta}$ will increase towards $\tilde{\Delta}_{\rm eq}$, thus negating the effect of the initial-perturbation decrease in Δ.

In contrast, if $\eta'(j_0) > \xi\eta'(j_*) > 0$, then l_η is reduced by a larger factor than Δ; thus the resulting perturbed Petschek configuration has $\tilde{\Delta} > \tilde{\Delta}_{\rm eq} = K\tilde{l}_\eta$. Invoking again the results of numerical simulations, we conclude that the system will evolve in such a way as to decrease $\tilde{\Delta}$ further. In fact, this scenario describes what happens in the case of solution I, but its application to this solution involves some subtlety. Indeed, notice that one can use equations (19) — (24) only if $\eta'(j_*) \neq 0$. Thus, in order to apply this general analysis to solution I, we need to modify the function $\eta(j)$ slightly to make it monotonically increasing in the region $j < j_c$. In other words we tentatively assume that this function has a non-zero positive (although arbitrarily small) slope $\eta'(j) > 0$ in this region. This modification is not essential; it needs to be introduced here purely for our technical convenience, to be able to use our general equations (19) — (24). We do not actually need to rely on it in order to derive the same conclusions regarding solution I. Indeed, if we insist on our unmodified function $\eta(j)$ with the slope $\eta'(j)$ being exactly equal to zero for $j < j_c$, then, instead of equations (19)—(24), we can use an alternative argument to describe the response of solution I to the initial perturbation. This argument is in fact even simpler and physically more transparent than the one described above; it goes as follows.

Since j_0 in solution I lies on the steeply rising part of the $\eta(j)$ dependence, the central resistivity is increased by a relatively large amount given by equation (14). On this part of the curve, we have $\eta'(j_0) \simeq \eta_1/\Delta j$, and so

$$\eta(\tilde{j}_0) = e\eta_0 + \epsilon\eta_1 \frac{j_0}{\Delta j}\,. \tag{25}$$

Then, $\eta(\tilde{l}_\eta) \equiv \eta(\tilde{j}_0)/e = \eta_0 + \frac{\epsilon}{e}\eta_1(j_c/\Delta j)$, and, therefore, $j_* \in [j_c, \tilde{j}_0]$, i.e., $\tilde{j}_* \approx \tilde{j}_0$. If the perturbed current density $\tilde{j}(y)$ has a characteristic scale $\tilde{\Delta}$, then $\tilde{j}_* \approx \tilde{j}_0$ implies that $\tilde{l}_\eta \ll \tilde{\Delta}$. Thus we see that, as the principal effect of the initial perturbation, the size $\tilde{l}_\eta$ of the resistivity enhancement region drops very sharply, whereas all other quantities change rather smoothly. Then we can again invoke our empirical fact that a configuration like this will not stay stationary but will evolve so that the current layer width $\tilde{\Delta}$ will tend to decrease to become comparable with $\tilde{l}_\eta$, in agreement with our expectations.

But as $\tilde{\Delta}$ changes during the subsequent evolution for $t > 0$, there will be a feedback on $\tilde{\delta}$.

Indeed, since the diffusion region always remains a Sweet–Parker layer, $\tilde{\delta}$ and $\tilde{\Delta}$ are always related via equation (6). Since $\eta(j_0)$ is a monotonically increasing function of $j_0 \propto 1/\delta$, we see that $\tilde{\delta}$ is a monotonically increasing function of $\tilde{\Delta}$. For example, for solution I, we can, using the fact that $\tilde{j}_0$ is always very close to j_c, approximate $\tilde{\delta}$ by δ_c everywhere except where it appears in the combination $(\delta_c - \tilde{\delta})$. We thus can express the resistivity as $\eta(\tilde{j}_0) \simeq \eta_1(j_c/\Delta j)(\delta_c - \tilde{\delta})/\delta_c$ and, substituting this expression into equation (6), obtain

$$\left(\frac{\delta_c - \tilde{\delta}}{\delta_c}\right)^I = \frac{\delta_c}{\tilde{\Delta}} \frac{V_A \delta_c}{\eta_1} \frac{\Delta j}{j_c} \,. \tag{26}$$

We thus see that the decrease in $\tilde{\Delta}(t)$ leads to a proportional increase in $\delta_c - \tilde{\delta}(t)$. In a similar manner, for solution II we find, using equations (6) and (7), that $\tilde{\delta} \propto \tilde{\Delta}^{1/3}$. In either case we see that after the initial perturbation, the subsequent evolution of the system is such that δ changes in the same direction as Δ.

Now we are ready to apply the above general results to the issue of stability of our solutions I and II. We see that in the case of solution I, the initial decrease in δ and Δ tends to amplify further. This means that this solution is unstable: a slight increase in j_0 will lead to further increase and thus the system will move away from the initial equilibrium, towards higher values of central current density and resistivity, until it approaches solution II.[2] Solution II, on the other hand, is stable; indeed, as have shown above, after its initial decrease [equation (17)], Δ and hence δ will tend to increase, thereby reducing the initial perturbation. Thus, in this case the feedback is negative and hence solution II is stable.

It is important to realize that, in practice, solution I is likely to be irrelevant for another reason (in addition to being unstable). Indeed, real astrophysical systems, including solar flares, always have a finite (albeit very large) global size L. For the Petschek model to work, we must have $\Delta \leq L$. This condition imposes an upper limit on Δ and hence, via equation (6), a lower limit on $\eta(j_0)$. For example, for j_0 on the rapidly rising part of the $\eta(j)$ curve, this condition can be cast as

$$\eta(j_0) > \eta_{\min}(L) \equiv \frac{\delta_c^2 V_A}{L} \,. \tag{27}$$

If $\eta_{\min} > e\eta_0$, then solution I does not even exist for a given global size L. For typical solar corona conditions, collisional resistivity η_0 is so small that inequality (27) is not satisfied; in other words, one gets a very large value for Δ^I, much larger than $L \simeq 10^9$ cm.

---

[2]At the same time, a slight initial decrease in j_0 will presumably lead to a further decrease in j_0 and hence an increase in Δ, until the system reaches the stable Sweet–Parker configuration with $\Delta = L$ and $\eta(j_0) = \eta_0$. This scenario, however, can only occur if the system's size L is tremendously large; it is therefore of no importance to solar flares, as discussed below [see equation (27)].

Here is how the requirement that $\eta(j_0) > \eta_{\min}(L)$ comes into play from the evolutionary point of view. As a reconnection layer starts to form, its thickness decreases rapidly until it reaches δ_c; after that, δ and the central current density j_0 both stay approximately constant while $\eta(j_0)$ increases rapidly. When $\eta(j_0)$ reaches $\eta_{\min}$, the corresponding width Δ of the diffusion region, determined by equation (6), becomes equal to L. From this moment on, the reconnection system can be described by the Petschek model. The particular Petschek configuration found exactly at this moment (i.e., when $\eta = \eta_{\min}$ and hence $\Delta = L$) is that of Sweet–Parker. If $\eta_{\min} > e\eta_0$, then $j(l_\eta) > j_c$ and hence is very close to j_0; this means that resistivity is very strongly localized, $l_\eta \ll \Delta$. Therefore, this configuration will not be at equilibrium, and the system will evolve through a sequence of Petschek configurations with ever-increasing j_0 and $\eta(j_0)$. Each of these configurations with j_0 on the rapidly rising part of the $\eta(j)$ curve will have $\Delta > \Delta_{\rm eq} = Kl_\eta$ until the configuration corresponding to the stable equilibrium solution II is reached.

We have thus demonstrated that a physical system with anomalous resistivity of the type shown on Figure 1 will evolve towards a stable solution II, which is characterized by the following values of the central current density and resistivity:

$$j_0 \simeq ej_c/\xi\,, \tag{28}$$

$$\eta(j_0) \simeq e\eta_1/\xi\,. \tag{29}$$

The exact coefficients in these expressions require a precise model for $\eta(j)$, etc...

Finally, let us make a couple of remarks regarding our choice of ξ. In the above considerations we have assumed that $\xi > 1$. Notice that the case $\xi = 1$ ($\Delta_{\rm eq} = l_\eta$) is, in a certain sense, degenerate: in addition to an unstable solution I, one gets a continuum of neutrally stable solutions II that correspond to $j_0 \geq ej_c$. Our present analysis does not allow us to discriminate among these solutions; they all appear to be equally plausible. If, however, one considers the unique stable solutions II with $\xi > 1$ and takes the limit $\xi \to 1$, then one arrives at a single limiting solution (having $j_0 = ej_c$). Thus, we use this limiting solution to extend our family of solutions with $\xi > 1$ to include the $\xi = 1$ case.

However, if $\xi < 1$ ($\Delta_{\rm eq} < l_\eta$), then our present analysis does not work: one still has an unstable solution I, but no solutions of type II exist, at least as long as $\eta(j)$ remains a linear function. This suggest that the system will continuously evolve towards higher and higher values of j_0 and $\eta(j_0)$ and hence the reconnection process will continuously accelerate until some new resistivity saturation mechanism sets in. In this case, the system will stabilize and a steady state will be achieved at a much higher level of j_0 than the level $j_0 \sim j_c$ discussed here.

2.3. Reconnection Rate

Thus, we now have a stable steady state Petschek-like configuration with the central diffusion region characterized by the thickness $\delta \simeq \delta_c/\zeta$ and the central resistivity $\eta = \zeta\eta_1$. Here, ζ is a finite constant; according to our analysis, $\zeta = e/\xi$. However, we realize that the simple qualitative model presented here is not adequate for providing any numerical accuracy; it should only be used for order-of-magnitude estimates. Therefore, in the following we shall just keep using the above expressions for δ and $\eta(j_0)$, parameterizing our ignorance by a constant $\zeta = O(1)$.

Let us now ask, what is the reconnection rate associated with this configuration? Using expression (4) we find the aspect ratio of the central diffusion region:

$$\frac{\Delta}{\delta} = \frac{V_A\delta}{\eta(j_0)} = \frac{S_*}{\zeta^2}\,, \tag{30}$$

where we define

$$S_* \equiv \frac{V_A\delta_c}{\eta_1}\,. \tag{31}$$

[Note: the parameter S_* defined here is completely different from Kulsrud's (2001) S^*.]

The reconnection velocity is (assuming that the density stays roughly constant inside the reconnection layer):

$$\frac{V_{\rm rec}}{V_A} = \frac{\delta}{\Delta} = \zeta^2 S_*^{-1}\,, \tag{32}$$

and the typical reconnection timescale is

$$\tau_{\rm rec} \equiv \frac{L}{V_{\rm rec}} = \tau_A(L)\, S_*/\zeta^2\,, \tag{33}$$

where $\tau_A(L) \equiv L/V_A$ is the global Alfvén crossing time.

Note that the aspect ratio (30) and hence the reconnection velocity (32) turn out to be independent of the global system size L, but only depend on the local plasma parameters.

Also note that our expression (32) for the reconnection velocity differs from the result $V_{\rm rec}/V_A \sim (\delta_c\eta^*/V_AL^2)^{1/3}$ obtained previously by Kulsrud [see equation (26) of Kulsrud 2001]. We believe that this discrepancy can be attributed, at least partly, to a somewhat different functional form of the $\eta(j)$-dependence adopted in his paper.

3. Petschek Reconnection in the Presence of Anomalous Resistivity due to Ion-Acoustic Turbulence (IAT)

In this section we assume that the anomalous resistivity enhancement is caused by the scattering of the current-carrying electrons off ion-acoustic waves, which are themselves excited by the ion-acoustic instability when the current density exceeds a certain threshold. The theory of ion-acoustic turbulence and the associated with it anomalous resistivity has greatly progressed over the past 40 years (e.g., Kadomtsev 1965; Rudakov & Korablev 1966; Sagdeev 1967; Tsytovich & Kaplan 1971; Biskamp & Chodura 1972; Coroniti & Eviatar 1977; Bychenkov et al. 1988). This theory is now very mature and seems to be capable of producing reliable quantitative results regarding anomalous resistivity. In this paper, we use the results presented by Bychenkov et al. (1988).[3]

Following the analysis of ion-acoustic turbulence by Bychenkov et al. (1988), we adopt

$$j_c = a_1 e n_e v_s \,, \tag{34}$$

where $v_s \equiv \sqrt{ZT_e/m_i}$ is the ion sound speed, and $a_1 = O(1)$. In particular, according to equation (2.143) of Bychenkov et al. (1988), $a_1 \simeq 2.14$.

Further, we compute anomalous resistivity $\eta(j > j_c + \Delta j)$ by using the expression (2.148) of Bychenkov et al. (1988) for $\sigma = \sigma_{\rm anom}(E)$ to express $\eta = c^2/4\pi\sigma$ in terms of the electric current density $j = \sigma E$. We thus obtain[4]

$$\eta(j) \simeq \frac{1}{4\pi \cdot 0.16} \frac{c^2}{\omega_{pe}^2} \left(\frac{\lambda_{De}}{\lambda_{Di}}\right)^2 \frac{j}{\sqrt{8\pi n_e T_e}} \simeq \frac{1}{36} \frac{c^2}{\omega_{pe}} \frac{ZT_e}{T_i} \sqrt{\frac{Zm_e}{m_i}} \frac{j}{en_e v_s} \,. \tag{35}$$

We then estimate η_1 by extrapolating this dependence down to $j = j_c + \Delta j \simeq j_c$. Using equation (34), we get

$$\eta_1 = \eta(j_c) = a_2 \frac{c^2}{\omega_{pe}} \frac{ZT_e}{T_i} \sqrt{\frac{Zm_e}{m_i}} \,, \tag{36}$$

where

$$a_2 \simeq \frac{a_1}{36} \simeq 0.06 \,. \tag{37}$$

---

[3]We note, however, that here we use the results of the theory of ion-acoustic anomalous resistivity that has been developed for a homogeneous plasma without magnetic field. We acknowledge that the resistivity may be modified by both the presence of the magnetic field and by the fact that in our analysis turbulence is presumed to be confined to the very small central diffusion region, and is thus strongly inhomogeneous.

[4]Note that the value for anomalous conductivity given by Bychenkov et al. (1988) differs by a numerical factor of order one from the famous Sagdeev's (1967) formula.

For a pure hydrogen plasma ($Z = 1$, $m_i = m_p$), we have:

$$\eta_1 = 1.4 \cdot 10^{-3} \frac{c^2}{\omega_{pe}} \frac{T_e}{T_i} \,. \tag{38}$$

As for η_0, we take it to be the classical collisional Spitzer resistivity

$$\eta_0 \equiv \eta_{\rm Sp} = \frac{c^2}{4\pi\sigma_{\rm Sp}} \simeq \frac{0.02\Lambda}{N_D} \frac{c^2}{\omega_{pe}} \,, \tag{39}$$

where Λ is the Coulomb logarithm and

$$N_D \equiv n_e \lambda_{De}^3 \,, \tag{40}$$

$\lambda_{De} \equiv \sqrt{T_e/4\pi n_e e^2}$ being the electron Debye radius. We see that we may expect a potential resistivity enhancement on the order of

$$\frac{\eta_1}{\eta_{Sp}} = \frac{N_D}{2\Lambda} \frac{T_e}{T_i} \sqrt{\frac{m_e}{m_i}} \gg 1. \tag{41}$$

For this model of anomalous resistivity, δ_c and η_1 are given by expressions (8) and (36) and then we can express S_* as

$$S_* = \frac{1}{a_1 a_2} \frac{V_A^2}{c v_s} \frac{T_i}{Z T_e} \frac{m_i}{Z m_e} \,. \tag{42}$$

Expressing the ratio V_A/v_s in terms of the composite electron plasma beta parameter,

$$\beta_e \equiv \frac{8\pi n_e T_e}{B_0^2} \,, \tag{43}$$

as $V_A/v_s = \sqrt{2/\beta_e}$, we can rewrite (42) as

$$S_* = a_3 \frac{V_A}{c\sqrt{\beta_e}} \frac{T_i}{Z T_e} \frac{m_i}{Z m_e} \,, \tag{44}$$

where

$$a_3 \equiv \frac{\sqrt{2}}{a_1 a_2} \simeq 11 \,, \tag{45}$$

where we substituted $a_1 = 2.14$ and made use of equation (37).

Note that from equations (8) and (34) it easily follows that

$$\frac{\delta_c}{d_i} = \frac{1}{a_1} \sqrt{\frac{2}{\beta_e}} \,, \tag{46}$$

where

$$d_i \equiv \frac{c}{\omega_{pi}} \tag{47}$$

is the ion skin depth. Substituting this very useful expression, along with equation (44), into our equation (30) for Δ, we find

$$\Delta \simeq \frac{a_4}{\zeta^3}\, d_i\, \frac{m_i}{Zm_e}\, \frac{T_i}{ZT_e}\, \frac{V_A}{c\beta_e}\,, \tag{48}$$

where

$$a_4 \equiv \frac{2}{a_1^2 a_2} \simeq 7.3\,. \tag{49}$$

We also get an expression for the Alfvén crossing time for the diffusion region — one of the most important timescales in the problem:

$$\tau_A(\Delta) \equiv \frac{\Delta}{V_A} \simeq \frac{a_4}{\zeta^3}\, \omega_{pi}^{-1}\, \beta_e^{-1}\, \frac{m_i}{Zm_e}\, \frac{T_i}{ZT_e}\,. \tag{50}$$

In addition, substituting equation (44) into equation (33) for the reconnection time $\tau_{\rm rec}$, we find a very simple relationship expressing $\tau_{\rm rec}$ in terms of the light crossing time L/c and β_e:

$$\tau_{\rm rec} \simeq \frac{a_3}{\zeta^2\sqrt{\beta_e}}\, \frac{L}{c}\, \frac{T_i}{ZT_e}\, \frac{m_i}{Zm_e}\,. \tag{51}$$

For a pure hydrogen plasma ($Z = 1$, $m_i = m_p = 1836\, m_e$), we get

$$S_* \simeq 2\cdot 10^4 \frac{V_A}{c\sqrt{\beta_e}}\, \frac{T_i}{T_e}\,, \tag{52}$$

$$\Delta \simeq 1.3\cdot 10^4 \zeta^{-3}\, d_i \frac{T_i}{T_e}\, \frac{V_A}{c\beta_e}\,, \tag{53}$$

$$\tau_A(\Delta) \simeq 1.3\cdot 10^4 \zeta^{-3}\, \omega_{pi}^{-1}\, \frac{T_i}{T_e}\, \beta_e^{-1}\,, \tag{54}$$

$$\tau_{\rm rec} \simeq \frac{2\cdot 10^4}{\zeta^2\sqrt{\beta_e}}\, \frac{L}{c}\, \frac{T_i}{T_e}\,. \tag{55}$$

Note that in all these expressions n_e and T_e are to be taken at the *center* of the reconnection layer ($x = y = 0$), while the magnetic field B_0 is the reconnecting magnetic field *outside* the layer, at $x > \delta$, $y = 0$.

4. Application to Solar Flares

Let us now try to apply the above results to typical solar flare conditions and see whether our model is able to explain the very short time scale of impulsive flares. In order to be able to make quantitative estimates, we shall first need to discuss the values of some relevant plasma parameters.

Table 1 lists the values of the key parameters of our model, along with the values of some fundamental plasma parameters, for two sets of conditions. Both sets are calculated for fully-ionized pure hydrogen plasma. The first set (column III) illustrates the fiducial solar coronal conditions: $B_0 = 100$ G, $n_e = 10^9$ cm^{-3}, and $T_e = T_i = 2 \cdot 10^6\, K \simeq 200$ eV. The second set (column IV) corresponds to the fiducial solar flare conditions which will be discussed below.

For the parameters in column III we see that the characteristic reconnection time turns out to be no more than an order of magnitude longer than the observed flare duration time (which is typically of order 10^3 sec), but it is, apparently, still not sufficiently short. Notice, however, that the fiducial solar corona parameters used in column III may not be appropriate for the center of the solar flare reconnection layer. Indeed, one can expect that the turbulence will lead to rapid heating of the plasma, resulting in a substantial rise of the electron temperature.

We can then ask whether the electron thermal pressure at the center of the current layer will grow to a level where it becomes comparable to the outside magnetic pressure, $\beta_e = O(1)$. This is a very important question because, according to equation (46), the value of β_e controls the regime that the system finds itself in. In particular, if $\delta < d_i$, then the diffusion region needs to be described in terms of electron MHD (or Hall MHD), the theory of which in the reconnection context has recently been greatly advanced by a number of researchers (e.g., Drake et al. 1994; Biskamp 1997; Bhattacharjee et al. 2001). Thus, we see that β_e is a very important parameter, whose value may have a profound influence on the applicability of the anomalous resistivity model adopted in this paper. Let us now ask what value for β_e one can expect in the case of magnetic reconnection in solar corona.

First, notice that it seems inevitable that, if there is no axial (or guide) magnetic field component, that is when $B_z = 0$, then one has to have $\beta_e = O(1)$. Indeed, in this case the basic requirement of pressure balance across the current layer dictates that the plasma pressure at the center of the layer's diffusion region be equal to the pressure of the magnetic field outside of the layer. This means that $\beta_e = 1$ when $T_e \gg T_i$ (and hence the ion pressure inside the layer is negligible) and $\beta_e = 1/2$ when $T_i = T_e$ (and hence the ion pressure is equal to the electron pressure for pure hydrogen plasma). This conclusion holds regardless

of the energy budget balance. For example, if there is no effective cooling mechanism, then the electron density n_e does not change significantly (i.e., by more than a factor of order one), whereas the temperature increases up to the "equipartition level", $T_{\rm eq} = B_0^2/8\pi n_e$, which is about $3 \cdot 10^8$ K for $n_e = 10^{10}$ cm^{-3} and $B_0 = 100$ G. On the other hand, if there is some effective cooling, the plasma temperature cannot reach such a high value and then the density is increased instead to maintain the pressure balance across the layer. In either case, one finds $\beta_e = O(1)$ and hence, according to equation (46), $\delta \sim d_i$. This means that the system will require a Hall-MHD description as soon as, or even before, the anomalous resistivity becomes important.

In the case of solar flares, however, it is unclear whether this situation is present. Indeed, there exist a possibility for maintaining the pressure balance across the layer with $\beta_e \ll 1$. This scenario requires two things, both likely to be relevant in solar flare environment: the presence of a non-zero axial component of the magnetic field B_z and some plasma cooling mechanism. Indeed, when the plasma is cooled efficiently, the increase in thermal pressure that is required to maintain the pressure balance cannot come from the increase in temperature, and so the plasma tends to compress inside the reconnection layer. This, in turn, leads to the proportional compression of the guide field component (here we are neglecting the resistive decoupling between the guide field and the plasma):

$$\frac{B_z|_{\rm inside}}{B_z|_{\rm outside}} = \frac{n_e|_{\rm inside}}{n_e|_{\rm outside}}\,. \tag{56}$$

(Here the subscript "inside"corresponds to the center of the reconnection layer, $x = y = 0$, whereas the subscript "outside" corresponds to the plasma above the layer, $y = 0$, $x \gg \delta$.)

If cooling is so strong that the resulting central temperature is small compared with the equipartition temperature, then the plasma pressure can be neglected in the pressure balance. The pressure balance is then achieved with the increased guide field pressure inside the layer balancing the reconnecting field's pressure outside the layer:

$$B_z^2|_{\rm inside} - B_z^2|_{\rm outside} = B_0^2\,. \tag{57}$$

Thus, $B_z|_{\rm inside}$ is determined from the pressure balance (57) and then the ratio $B_z|_{\rm inside}/B_z|_{\rm outside}$ determines the compression factor and hence the central density $n_e|_{\rm inside}$. Typically one might expect $B_z|_{\rm outside} \sim B_0$, and so B_z (and hence n_e) is increased at the center of the layer by a factor of order one. As for the central electron temperature, it is going to be determined by the balance between the turbulent ohmic heating and the cooling due to electron thermal conduction.[5] This is an important and very complicated problem and its detailed treatment

[5]In the context of solar flares the radiative cooling of the diffusion region, including both the

lies outside the scope of this paper. Therefore, here we shall give only some very simple estimates.

The characteristic ohmic heating time can be evaluated as

$$\tau_{\rm heat} \sim \frac{n_e T_e}{Q}\,, \tag{58}$$

where the ohmic heating rate per unit volume roughly is

$$Q \sim \frac{j_0^2}{\sigma} \sim \frac{B_0^2}{4\pi}\frac{\eta(j_0)}{\delta^2} \sim \frac{B_0^2}{4\pi}\frac{1}{\tau_A(\Delta)}\,, \tag{59}$$

so that

$$\tau_{\rm heat} \sim \tau_A(\Delta)\beta_e\,, \tag{60}$$

where we have dropped numerical factors of order unity. We thus see again that, in the case where there is no cooling, a cold fluid element entering the reconnection layer will be heated up very rapidly; in fact, the total time that the element spends (and is being heated) inside the inner diffusion region [of order $\tau_A(\Delta)$] is long enough for the plasma thermal pressure to reach $\beta_e = O(1)$.

If there is efficient cooling due to electron thermal transport, then an absolute lower bound on the electron cooling time is set by the time it takes a freely streaming thermal electron to leave the inner diffusion region of size Δ:

$$\tau_{\rm cool}^{\rm min} \sim \frac{\Delta}{v_{\rm th,e}} \sim \tau_A(\Delta)\frac{1}{\sqrt{\beta_e}}\sqrt{\frac{m_e}{m_i}}\,. \tag{61}$$

Then, equating $\tau_{\rm cool}^{\rm min}$ and $\tau_{\rm heat}$, we get a lower bound on β_e:

$$\beta_e^{\rm min} \sim \left(\frac{m_e}{m_i}\right)^{1/3} \ll 1\,. \tag{62}$$

This is the regime that is illustrated in column IV of Table 1. Here, we use the following values of plasma parameters for our "fiducial solar flare conditions": $B_0 = 100$ G, $n_e = 10^{10}$ cm^{-3}, $T_e = 3\cdot 10^7\,K \simeq 3000$ eV, and $T_i = 3\cdot 10^6\,K \simeq 300$ eV, which correspond to $\beta_e \simeq 0.1$. The resulting reconnection time scale $\tau_{\rm rec}$ is of the order of a hundred seconds, which is fast enough to explain the observed very short duration of the impulsive phase of solar flares.

---

bremsstrahlung and cyclotron mechanisms, appears to be ineffective, as the characteristic radiative cooling time is much longer than the time $\tau_A(\Delta)$ that a fluid element spends inside the diffusion region.

An upper limit on $\tau_{\rm cool}$ is given simply by the time that a fluid element spends inside the inner diffusion region, i.e., the Alfvén transit time $\tau_A(\Delta)$. This corresponds to the upper limit $\beta_e^{\rm max} = O(1)$, just as in a situation without a guide magnetic field or without cooling. The electron temperature then grows to about the equipartition value $T_{\rm eq} \simeq 3 \cdot 10^8$ K (for $n_e = 10^{10}$ cm^{-3} and $B_0 = 100$ G).

Here are a few more numbers:
23, 45.32, 18650, -0.652. :)

Thus, we can constrain β_e to lie between $\beta_e^{\rm min} \sim 10^{-1}$ and $\beta_e^{\rm max} = O(1)$. We then see from equation (46) that even in the case of the lowest possible β_e, the thickness δ of the inner reconnection layer is roughly of the same order of magnitude as d_i. This suggests that the Hall-MHD regime is likely to be at least marginally important in the physics of solar flares. In this case the nature of anomalous dissipative processes may differ from the simple effective resistivity $\eta(j)$ due to ion-acoustic turbulence as described in § 3 and thus a more elaborate theory is needed.

Finally let us address one more question related to the applicability of the ion-acoustic regime. One can raise the objection that, in order to excite ion-acoustic instability, the condition $T_e \gg T_i$ needs to be satisfied; if instead the plasma is nearly isothermal, with $T_e \sim T_i$, then Buneman instability (Buneman 1959) can in principle be excited, but at a higher current-density threshold, $j_c^{\rm Buneman} \sim en_e v_{\rm th,e} \gg en_e v_s$. To address this problem, let us consider a plasma that initially (i.e., before the onset of reconnection) is isothermal. As the reconnection current layer is been formed, the current density in the layer gradually increases and finally reaches the Buneman instability threshold (calculated for the initial, relatively low temperature $T_{e,0} \sim 2 \cdot 10^6$ K). The subsequent development of the instability leads to anomalous turbulent heating (Sagdeev 1967; Biskamp & Chodura 1973; Bychenkov et al. 1988; Kingsep 1991), which raises the electron temperature faster than the ion temperature. At some point, the electron temperature becomes much higher than the ion temperature and the ion-acoustic instability is excited. Such a transition from the Buneman regime to the ion-acoustic regime has in fact been studied previously (see Bychenkov et al. 1988 and references therein). In magnetic reconnection context, a possibility of this transition has recently been discussed briefly by Roussev et al. (2002). One complication, however, is that, since the plasma is constantly moving through the vicinity of the neutral point, then, in order to sustain the IAT, one needs to pre-heat the electrons (relative to the ions) in every fluid element that is just entering the diffusion region. This means that some sort of anomalous heat leakage across the magnetic field is probably needed. Whether and how this can be achieved is a difficult question, which falls outside of the scope of the present study.

5. Conclusions

In this paper we have presented a model of magnetic reconnection in the presence of a current-driven enhanced anomalous resistivity. This is a very simplistic, crude model that aims at predicting the qualitative behavior of the system and the scaling of the reconnection rate with various plasma parameters, while treating numerical factors of order one only very approximately.

In this model we have combined the following three ingredients. The first one is the observation, derived from several recent resistive-MHD numerical simulations (Erkaev et al. 2000, 2001; Biskamp & Schwarz 2001), that whenever the resistivity is strongly localized, the reconnecting system will develop a Petschek-like configuration, with the width of the inner diffusion region of the order of the resistivity localization scale. The second ingredient of our model is the Sweet–Parker model (Sweet 1958; Parker 1957, 1963) for the diffusion region of a Petschek configuration (Petschek 1964). Finally, the third ingredient is a physically realistic model for a current-driven anomalous resistivity expressed as a function $\eta(j)$, which exhibits two characteristic features. The first feature is a sudden jump of η from a small collisional value η_0 to a much larger value η_1 as soon as j exceeds a threshold j_c. The second feature is a subsequent linear growth $\eta \propto j$ for $j > j_c$. This choice is motivated by the theory of anomalous resistivity due to ion-acoustic turbulence, which has been developed in detail over the last 40 years (see, e.g., Bychenkov et al. 1988).

Note that the anomalous resistivity function adopted in this paper becomes very sensitive to electric current density when the latter exceeds some threshold value j_c; this makes it possible for the resistivity to be enhanced only in a small region, which, in turn, leads to the development of a Petschek-like configuration. Thus, our model is characterized by a reconnection rate that is enhanced (with respect to the classical, collisional-resistivity Sweet–Parker rate) by a combined action of anomalous resistivity and of the Petschek mechanism. It is important to realize that the role of anomalous resistivity in the acceleration of the reconnection process is two-fold: in addition to its direct action (lowering the global Lundquist number $S \equiv V_A L/\eta$), it accelerates reconnection indirectly, by turning on the Petschek mechanism.

The width of the inner diffusion region of the Petschek model, and thus the resistivity localization scale, are determined self-consistently when all the ingredients of the model are taken into account.

Based on our stability analysis of two possible Petschek-like states, we predict that the system will evolve towards a certain stable Petschek-like configuration. This stable configuration is characterized by the central current density j_0 and the central resistivity $\eta(j_0)$ exceeding j_c

and η_1, respectively, by a finite factor of order one. The reconnection velocity then scales as $V_{\rm rec} \sim V_A/S_* = \eta_1/\delta_c$, where $\delta_c = cB_0/4\pi j_c$ is the critical thickness of the layer.

We then consider (in § 3) the case of anomalous resistivity due to ion-acoustic turbulence, as an important specific example. We derive very simple expressions for the parameters of the reconnection system (e.g., the width Δ of the diffusion region, reconnection velocity $V_{\rm rec}$, and the reconnection time scale $\tau_{\rm rec}$) in terms of the basic plasma parameters n_e, T_e, T_i, and B_0.

Finally, in § 4, we apply our model to the solar flare environment. We note that reconnection process will lead to significant electron heating, so that the electron pressure at the center of the reconnection layer may become comparable to the pressure of the reconnecting magnetic field outside the layer. Based on our model, we obtain typical reconnection times of order $10^2 - 10^3$ sec; this is short enough to explain the very fast time scale of impulsive flares. We note however that, as a result of the plasma heating inside the reconnection layer, the thickness δ of the diffusion region quickly becomes comparable to, or even smaller than, the ion skin-depth, $d_i \equiv c/\omega_{pi}$. At these scales, new physical processes, described by Hall MHD, may come into play (Drake et al. 1994; Biskamp 1997; Bhattacharjee et al. 2001) even before the IAT develops and anomalous resistivity becomes important.

I am grateful to S. Boldyrev, H. Li, R. Kulsrud, and R. Rosner for some very helpful discussions and interesting comments. I would like to acknowledge the support by the NSF grant NSF-PHY99-07949.

REFERENCES

Bhattacharjee, A., Ma, Z. W., & Wang, X. 2001, Phys. Plasmas, 8, 1829.

Biskamp, D. 1986, Phys. Fluids, 29, 1520.

Biskamp, D. 1997, Phys. Plasmas, 4, 1964.

Biskamp. D. 2000, "Magnetic Reconnection in Plasmas", (Cambridge Univ. Press, New York, 2000).

Biskamp, D. & Chodura, R. 1973, Phys. Fluids, 16, 888.

Biskamp, D. & Schwarz, E. 2001, Phys. Plasmas, 8, 4729.

Buneman, U. 1959, Phys. Rev., 115, 503.

Bychenkov, V. Yu., Silin, V. P., & Uryupin, S. A. 1988, Phys. Reports, 164, 121.

Coppi, B., & Friedland, A. B. 1971, ApJ, 169, 379.

Coroniti, F. V. & Eviatar, A. 1977, Ap. J.Suppl., 33, 189.

Drake, J. F., Kleva, R. G., & Mandt, M.. E. 1994, Phys. Rev. Lett., 73, 1251.

Erkaev, N. V., Semenov, V. S., & Jamitzky, F. 2000, Phys. Rev. Lett., 84, 1455.

Erkaev, N. V., Semenov, V. S., Alexeev, I. V., & Biernat, H. K. 2001, Phys. Plasmas, 8, 4800.

Giovanelli, R.G. 1946, Nature, 158, 81.

Ji, H., Yamada, M., Hsu, S., & Kulsrud, R. 1998, Phys. Rev. Lett., 80, 3256.

Ji, H., Yamada, M., Hsu, S., Kulsrud, R., Carter, T., & Zaharia, S. 1999, Phys. Plasmas, 6, 1743.

Kadomtsev, B. B. 1965, Plasma Turbulence (New York: Academic Press)

Kadomtsev, B. B. 1975, Sov. J. Plasma Phys., 1, 389.

Kingsep, A. S. 1991, Sov. J. Plasma Phys., 17, 342

Kulsrud, R. M. 1998, Phys. Plasmas, 5, 1599.

Kulsrud, R. M. 2001, Earth, Planets and Space, 53, 417.

Parker, E. N. 1957, J. Geophys. Res., 62, 509.

Parker, E. N. 1963, ApJ Supplement, 8, 177.

Petschek, H. E. 1964, AAS-NASA Symposium on Solar Flares, (National Aeronautics and Space Administration, Washington, DC, 1964), NASA SP50, 425.

Rosner, R., Golub, L., Coppi, B., & Vaiana, G. S. 1978, ApJ, 222, 317

Roussev, I., Galsgaard, K., & Judge, P. G. 2002, A&A, 382, 639.

Rudakov, L. E. & Korablev, L. V. 1966, Sov. Phys. — JETP, 23, 145.

Sagdeev, R. Z. 1967, Proc. Symp. Appl. Math., 18, 281.

Sato, T. & Hayashi, T. 1979, Phys. Fluids, 22, 1189.

Scholer, M. 1989, J. Geophys. Res., 94, 8805.

Smith, P. F. & Priest, E. R. 1972, ApJ, 176, 487.

Sweet, P. A. 1958, in "Electromagnetic Phenomena in Cosmical Physics", ed. B.Lehnert, (Cambridge University Press, New York, 1958), p. 123.

Tsuneta, S. 1996, ApJ, 456, 840.

Ugai, M. & Tsuda, T. 1977, J. Plasma Phys., 17, 337.

Ugai, M. 1986, Phys. Fluids, 29, 3659.

Ugai, M. 1992, Phys. Fluids B, 4, 2953.

Ugai, M. 1999, Phys. Plasmas, 6, 1522.

Ugai, M. & Kondoh, K. 2001, Phys. Plasmas, 8, 1545.

Uzdensky, D. A. & Kulsrud, R. M. 2000, Phys. Plasmas, 7, 4018.

Vasyliunas, V. M. 1975, Rev. Geophys. Space Phys., 13, 303.

Yamada, M., Levinton, F. M., Pomphrey, N., Budny, R., Manickam, J., & Nagayama, Y. 1994, Phys. Plasmas, 1, 3269.

Yamada, M., Ji, H., Hsu, S., Carter, T., Kulsrud, R., Bretz, N., Jobes, F., Ono, Y., & Perkins, F. 1997, Phys. Plasmas, 4, 1936.

Yokoyama, T. & Shibata, K. 1994, ApJ Lett, 436, L197.

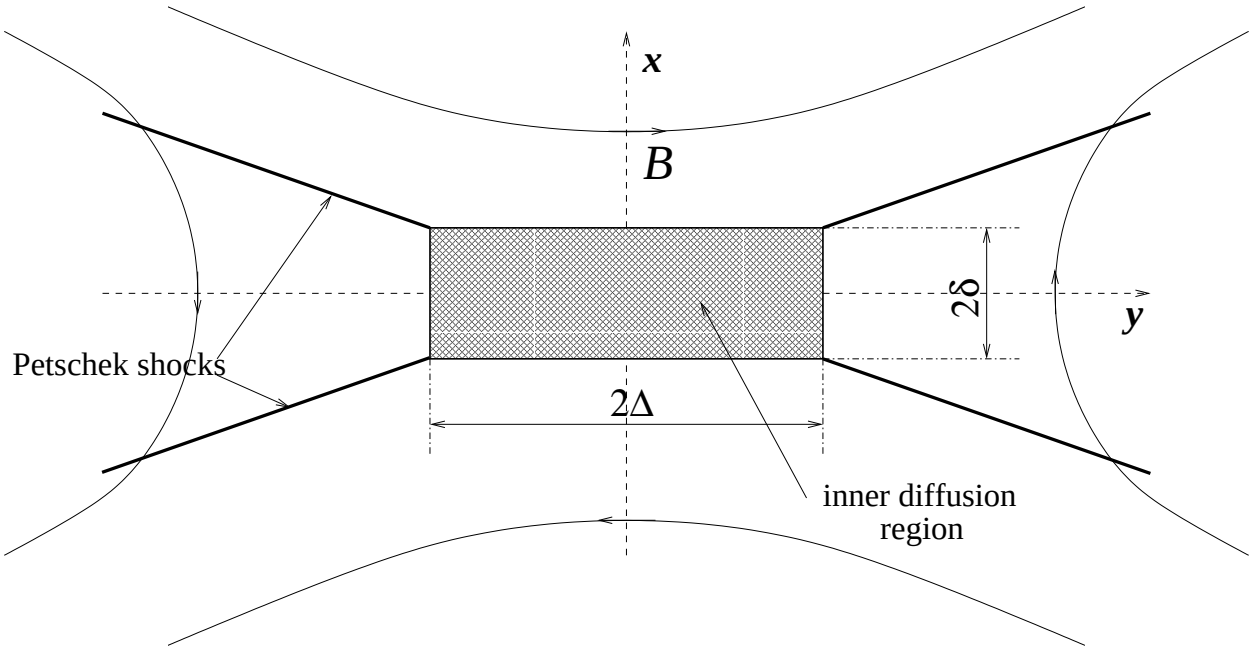

Fig. 1.— A schematic drawing of the inner diffusion region in the Petschek model.

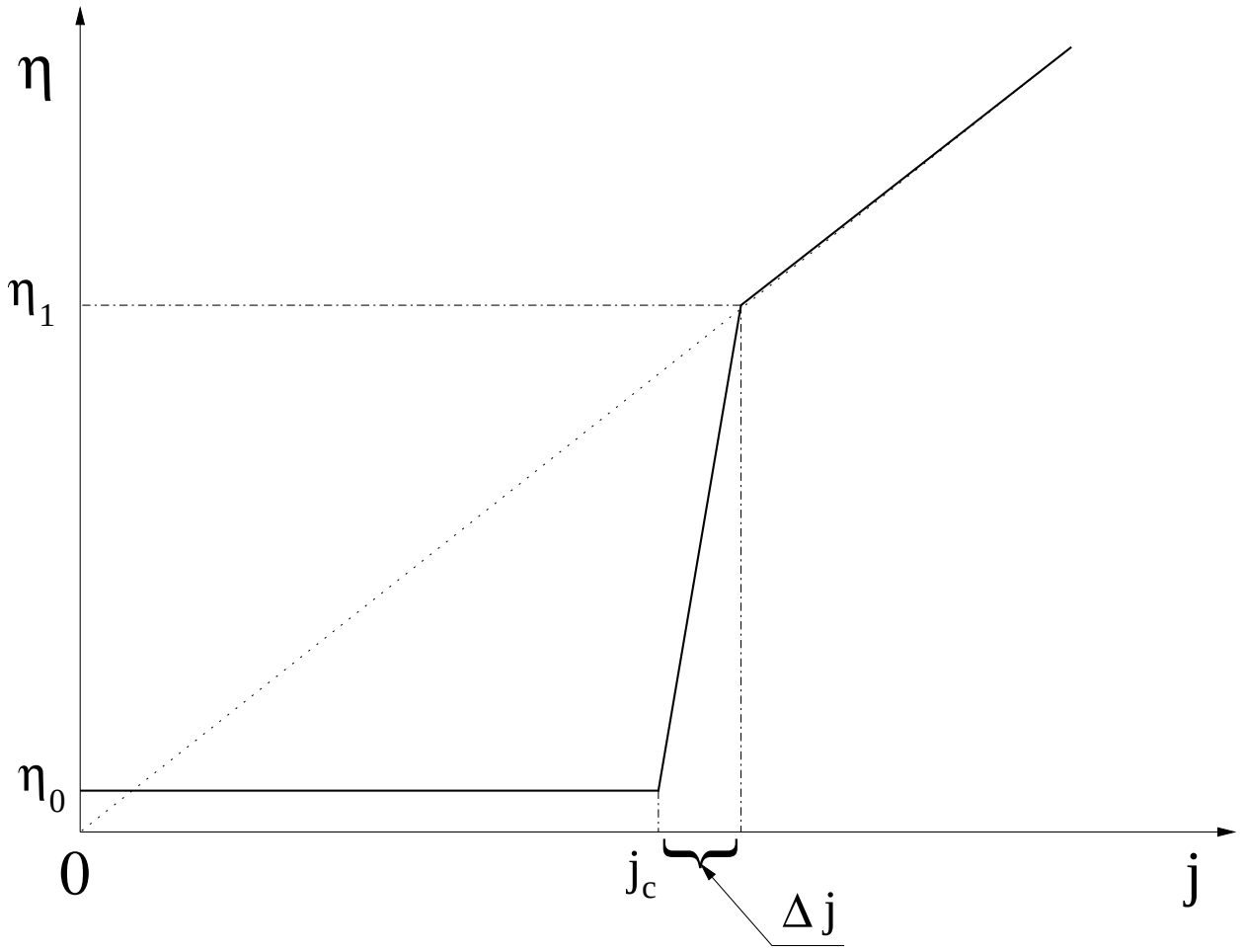

Fig. 2.— The anomalous resistivity model adopted in this paper.

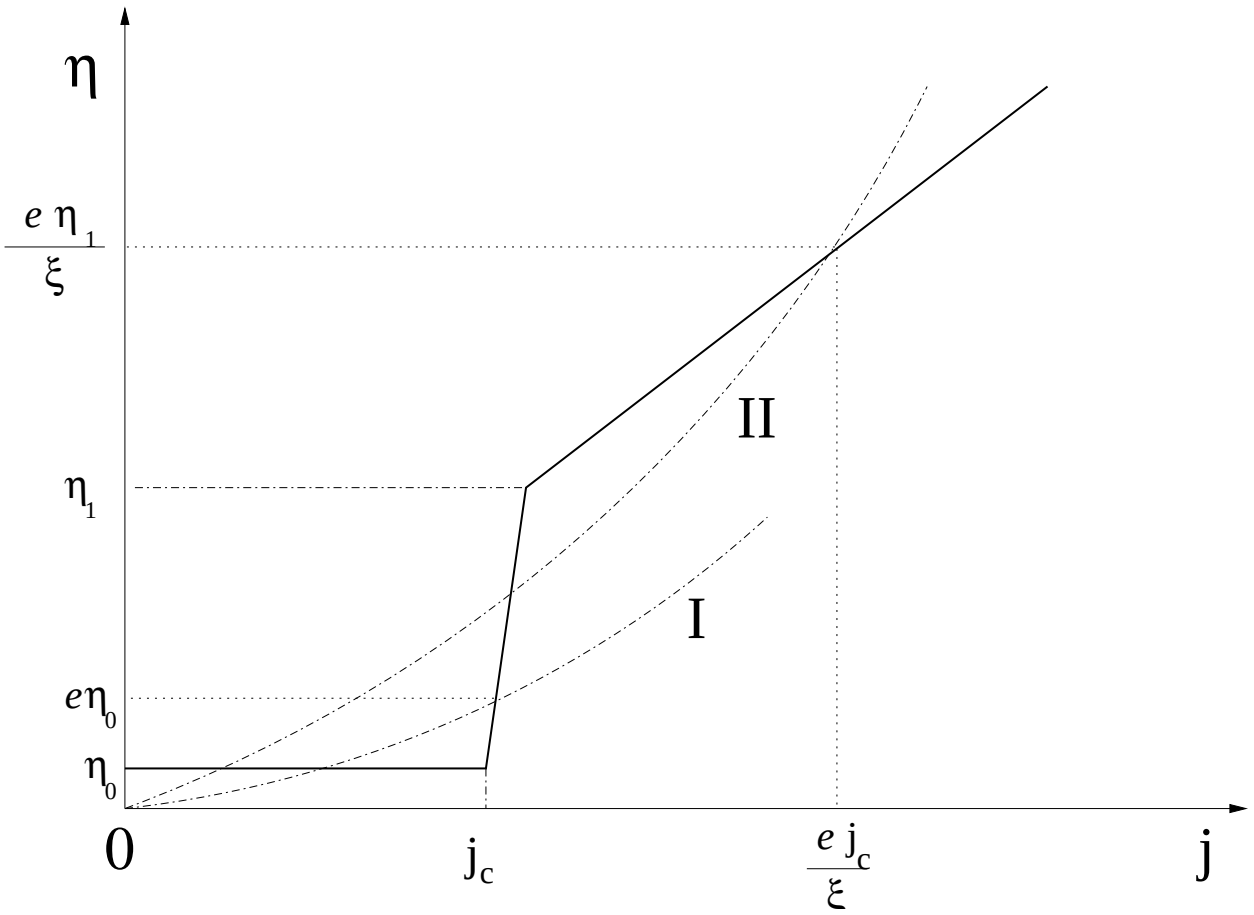

Fig. 3.— The two possible equilibrium solutions.

Table 1: Values of some basic plasma and reconnection region parameters in the typical coronal environment (column III) and in the flare environment (column IV). All values are calculated for pure hydrogen plasma ($Z = 1$, $m_i = m_p$) and for $\zeta = 2.0$ ($\xi = e/\zeta \simeq 1.36$); $\tau_{\rm rec}$ is calculated for $L = 10^9$ cm.

Parameter	Expression	Typical Coronal Value	Typical Flare Value
T_e, K	T_e	$2 \cdot 10^6$	$3. \cdot 10^7$
T_i, K	T_i	$2 \cdot 10^6$	$3. \cdot 10^6$
n_e, cm^{-3}	n_e	$1 \cdot 10^9$	$1 \cdot 10^{10}$
B_0, G	B_0	100	100
v_s, cm/sec	$\sqrt{T_e/m_p}$	$1.3 \cdot 10^7$	$5 \cdot 10^7$
V_A, cm/sec	$B_0/\sqrt{4\pi n_e m_p}$	$6.9 \cdot 10^8$	$2.2 \cdot 10^8$
ω_{pe}, sec^{-1}	$\sqrt{4\pi n_e e^2/m_e}$	$1.8 \cdot 10^9$	$5.6 \cdot 10^9$
ω_{pi}, sec^{-1}	$\sqrt{4\pi n_e e^2/m_p}$	$4.2 \cdot 10^7$	$1.3 \cdot 10^8$
Ω_e, sec^{-1}	$eB_0/m_e c$	$1.8 \cdot 10^9$	$1.8 \cdot 10^9$
Ω_i, sec^{-1}	$ZeB_0/m_p c$	$9.6 \cdot 10^5$	$9.6 \cdot 10^5$
λ_{De}, cm	$\sqrt{T_e/4\pi n_e e^2}$	0.31	0.38
λ_{Di}, cm	$\sqrt{T_i/4\pi n_e e^2}$	0.31	0.12
d_e, cm	c/ω_{pe}	17	5.3
d_i, cm	c/ω_{pi}	720	230
j_c, cgs-units	$2.14\ en_e v_s$	$1.3 \cdot 10^7$	$5.1 \cdot 10^8$
δ_c, cm	$cB_0/4\pi j_c$	$1.8 \cdot 10^4$	470
η_1, cm^2/sec	$1.4 \cdot 10^{-3}(T_e/T_i)c^2/\omega_{pe}$	$7.1 \cdot 10^8$	$2.2 \cdot 10^9$
β_e	$8\pi n_e T_e/B_0^2$	$7. \cdot 10^{-4}$	0.10
S_*	$2 \cdot 10^4 (T_i/T_e) V_A/c\sqrt{\beta_e}$	$1.7 \cdot 10^4$	45
Δ, cm	$\delta_c S_* \zeta^{-3}$	$4 \cdot 10^7$	$2.6 \cdot 10^3$
$\tau_A(\Delta)$, sec	Δ/V_A	0.057	$1.2 \cdot 10^{-5}$
$V_{\rm rec}$, cm/sec	$V_A \zeta^2/S_*$	$1.6 \cdot 10^5$	$1.9 \cdot 10^7$
E, cgs-units	$4\pi\zeta^2 j_c \eta_1/c^2$	$5.2 \cdot 10^{-4}$	$6.4 \cdot 10^{-2}$
$\tau_{\rm rec}$, sec	$L/V_{\rm rec}$	$6.3 \cdot 10^3$	52